

Phase Equilibrium of Hydrogen, Carbon Dioxide, Squalene, and Squalane[†]

Gerd Brunner,^{*,‡} Carla Saure,[§] and Dieter Buss^{||}

Institute for Thermal and Separation Processes, Hamburg University of Technology, Eissendorfer Str. 38, D-21073 Hamburg, Germany, Merck KgaA, Darmstadt, and EVONIK (Degussa-Hüls AG), Hanau

Squalene is applied in various fields of application. In contact with oxygen, it reacts to compounds with undesirable properties. Therefore, squalene often is hydrogenated to squalane, which is stable. Hydrogenation can advantageously be carried out with the additional application of supercritical carbon dioxide, which serves as a promoter for transporting hydrogen into the liquid phase and enhances equilibrium concentrations for squalane and squalene in the gaseous phase. In this paper, measurement and correlation of the relevant phase equilibrium data of the quaternary system are reported for search of optimized reaction conditions. In addition to literature data, VLE data are presented for the systems CO₂–squalane, CO₂–squalene, H₂–squalane, CO₂–H₂–squalene, and CO₂–H₂–squalene–squalane, in the temperature and pressure ranges of (310 to 350) K and (150 to 350) bar. The quaternary system CO₂–H₂–squalene–squalane and all subsystems can be correlated with cubic equations of state. For this work, the program package *PE*, available from the Institute for Thermal and Separation Processes, Hamburg University of Technology, was used, applying the Soave–Redlich–Kwong equation of state (SRK-EOS) with the Mathias–Klotz–Prausnitz (MKP) mixing rule. On the basis of measurements and on literature data, it is possible to correlate the experimental data and predict phase behavior in the process relevant ranges.

1. Introduction

Supercritical fluids have been investigated over the last 30 years extensively because their properties can be varied over a wide range by changes in pressure and temperature. This led to the development of new applications in separation processes and in reaction technology. Supercritical fluids allow the adjustment of selectivity in separation processes and the fine-tuning of reaction conditions which enables process optimization and intensification.¹ One of the chemical reactions which can be positively influenced by supercritical fluids is hydrogenation, in particular with the addition of supercritical carbon dioxide which enhances hydrogen transport to the liquid phase and the equilibrium concentrations of low volatile components in the gaseous phase. This led to the development of new hydrogenation processes for intermediates in the pharmaceutical industry. In this paper, the hydrogenation of squalene to squalane is the background for which reactions of the underlying phase equilibria of hydrogen, carbon dioxide, squalene, and squalane have been investigated and simulated.

Squalene is a ubiquitous substance in biochemistry. As a source, the liver oils of sea fishes are used, mainly from some shark species, the livers of which contain up to 80 % of squalene. Squalene occurs, in much lower concentrations, in olive oil, soya bean oil, wheat germ oil, palm oil, and many other oils from plants.² Squalane is the fully hydrogenated derivative of squalene. The structural formulas for both components are shown in Figure 1.

Squalene is applied in cosmetics, as a pharmaceutical agent, and as a nutraceutical.³ In contact with oxygen from air, it

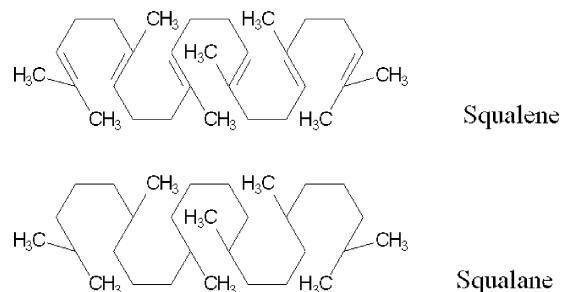


Figure 1. Structural formulas for squalene and squalane.

reacts to compounds with undesirable properties. Therefore, squalene often is applied in the hydrogenated form as squalane, which is stable and can thus be used as a main constituent of cosmetic products.

A number of investigations have been carried out to enrich squalene from various natural sources.^{5–8} They contain valuable information on the phase equilibrium of multicomponent systems but do not systematically investigate the phase behavior of hydrogen, carbon dioxide, squalane, and squalene and mixtures thereof.

Hydrogenation can advantageously be carried out with the additional application of supercritical carbon dioxide, which serves as a promoter for transporting hydrogen into the liquid phase and enhances equilibrium concentrations of squalane and squalene in the gaseous phase. It is the aim of this paper to provide the relevant phase equilibria data of the quaternary system and correlate them, to reduce the necessary experiments for determining the equilibria and to make available methods for careful extrapolations for the search of optimized reaction conditions.

* Corresponding author. Phone: +4940428783040. Fax: +4940428784072. E-mail: brunner@tu-harburg.de.

[†] Part of the "Gerhard M. Schneider Festschrift".

[‡] Hamburg University of Technology.

[§] Merck KgaA.

^{||} EVONIK (Degussa-Hüls AG).

Table 1. Data Sources in the Literature for Subsystems of Hydrogen, Carbon Dioxide, Squalene, and Squalane

system	data source	<i>T</i> [K]	<i>P</i> [MPa]
hydrogen–CO ₂	Tsang et al., 1980 ¹¹	220 to 290	up to 172
	Spano, J.O. et al., 1968 ²⁸	220 to 290	up to 20.3
	Bezanehtak, J. et al., ²⁹	278 to 308	1.5 to 19.2
hydrogen–squalane	Brunner, 1978 ¹³	327 to 423	30 to 87
	Löhrli-Thiel, 1978 ¹⁴		
	Kim et al. ¹⁵	295	0.7 to 1.4
hydrogen–CO ₂ –squalane	Brunner, 1978 ¹³	343 to 423	30 to 68
	Saure, 1996 ¹⁰	313 to 373	10 to 30
CO ₂ –squalene	Catchpole et al., 1997 ¹⁶	313 to 333	10 to 25
	Catchpole et al., 1998 ¹⁷	323 to 333	10 to 30
	Liphard, Schneider, 1975 ¹²	273 to 423	5 to 100
CO ₂ –squalane	Brunner, 1978 ¹³		
	Sovova et al., 1997 ¹⁸	303 to 328	7.9 to 27.5

Table 2. Physical Properties of the Used Substances

chemical formula	molecular weight [g·mol ⁻¹]	critical pressure <i>P</i> _C	critical temperature <i>T</i> _C	
		[MPa]	[K]	
squalene	C ₃₀ H ₅₀	410.70	1.11 ^a	782.13 ^a
squalane	C ₃₀ H ₆₂	422.83	1.13 ^a	822.89 ^a
carbon dioxide	CO ₂	44.1	7.38	304.15
hydrogen	H ₂	2.0	1.29	33.0

^a Values derived from fitting the Soave–Redlich–Kwong equation of state to vapor pressure data. For squalene from refs 2 and 3. Experimental values scatter; the value for the boiling temperature at ambient pressure was omitted due to inconsistency with the other vapor pressure data. For squalane, from refs 25 and 26.

2. Literature Data

The following survey has been accomplished with care. Nevertheless, there may exist published data on the subsystems, which have not been found. The data sources from the literature are summarized in Table 1, as far as they contain subsystems of the quaternary system of hydrogen, carbon dioxide, squalene, and squalane. These data have been used for planning the experimental investigation of the ternary and quaternary systems.

Earlier data^{12,13,28} were determined for acquiring knowledge on phase behavior and on experimental methods for determining high-pressure phase equilibria, while later work concentrated on the recovery of squalene or the purification of tocopherols by removal of squalene, in particular the work by Catchpole and co-workers,^{6,16,17} Ruivo et al.,⁷ and Vázquez et al.⁸ Sovova et al.¹⁸ and Bezanehtak, J. et al.²⁹ resumed thermodynamic interest in experimental and theoretical treatment.

In this work, phase equilibrium data were first determined as a basis for carrying out the hydrogenation of squalene to squalane in an atmosphere of hydrogen and carbon dioxide. Some experimental data were determined in this work for comparison to literature data to confirm the experimental procedure. In addition to the data measured specifically for the hydrogenation project, not yet published data on subsystems determined earlier in our laboratory were included. These combined data are reported in the following tables.

3. Experimental Determination of Phase Equilibrium for H₂, CO₂, Squalene, and Squalane

3.1. Materials. In Table 2 some properties of the substances used are listed. All chemicals were obtained from commercial sources, controlled by GC, and used in the delivered quality and not further purified. Carbon dioxide with a purity of better than 99.99 % was obtained from KWD, Bad Hönningen, Germany. Hydrogen was obtained from Air Products GmbH, Lüneburg, Germany, with a purity of 99.993 %. Squalene and squalane were obtained via a retailer from Merck AG, Darm-

stadt, Germany, or from Riedel-de Haën, Hannover, Germany, in p.a.-grade with purities > 99 %.

3.2. Experimental Method and Setup.⁹ For measuring phase equilibria, for this work an apparatus previously used by Stoldt and Brunner¹⁹ and modified by Pfohl²⁰ was applied, which used the static-analytical method. It was modified with additional autoclaves in contact with the main equilibrium autoclave to avoid pressure drop during sampling. The phase equilibrium apparatus used for most of the experiments is shown in Figure 2 and Figure 3. Some of the earlier experiments have been carried out in a very similar apparatus, missing only the buffer autoclaves.

The apparatus consists essentially of two autoclaves, which are immersed in a 100 dm³ liquid bath (heating liquid: Tellus C10, flash point 423 K, Shell, Hamburg, Germany) which is kept at constant temperature by a laboratory circulation thermostat (USG/R400, 3 kW, temperature deviation: 0.01 K, Lauda, Dr. R. Wobser, Lauda-Königshofen, Germany). The circulating liquid is evenly distributed in the liquid bath. The temperature in the bath was determined to vary less than ± 0.1 K. The main autoclave, shown schematically on the right-hand side in Figure 2, is the equilibrium cell from which the samples are taken. It has a volume of 1.2 dm³ (Haage, Mülheim, Germany; inner diameter 80 mm, steel No. 1.4571, metallic cone sealing). The equilibrium cell is equipped with a magnetically coupled stirrer (BR1, No. 6.138.187, Buddeberg, Mannheim, Germany, three blades) to enhance the approach of equilibrium. The smaller autoclave, to the left in Figure 2, has a volume of 0.3 dm³ and serves as a buffer autoclave. The third autoclave is placed outside the liquid bath and prevents liquid from flowing into the syringe-type pump. This pump (ISCO Division, Lincoln, NE, 260D, connected to a precision pressure transformer, No., 891.26.500, WIKA, Klingenberg/Main, Germany) keeps the pressure in the equilibrium cell and the buffer autoclave constant during sampling by introducing a gaseous mixture, corresponding to the one contained in the buffer autoclave. This causes some of the liquid phase of the buffer autoclave to flow (via valves V17 and V17') into the equilibrium cell. Since the liquid phases in both autoclaves are not different in composition within the limits of measurement, phase equilibrium in the equilibrium cell will not be disturbed, again within the limits of measurement.

After equilibrium was established and the phases were internally separated by gravity, samples were taken from the autoclave via capillaries of small diameter. Samples are taken from the equilibrium cell through three capillaries, diameter 0.25 mm, ending at 3 mm, 120 mm, and 225 mm below the lower side of the upper flange which is 238 mm above the bottom of the autoclave. The capillaries are heated outside the autoclave and insulated. Their temperature can be manually controlled. Samples are taken through the capillaries with valve nos. V8, V9, and V10. The sample valves (1/8", 10V208-TG, Autoclave Engineers, Erie, PA, USA) can be opened and closed slowly, enabling a careful sampling. The valves are also heated. At the outlet of the valves, capillaries of 100 mm length are attached which lead to the sampling vials (Figure 3 at the right-hand side).

The sampling apparatus is shown in Figure 3. In the sampling apparatus, the samples are separated into the condensable part and into a gaseous part. Samples were expanded via two glass tubes in sequence which were kept at 273 K with water and ice and about 200 K with an acetone–solid carbon dioxide heterogeneous mixture. Squalene and squalane were separated from the gases and liquefied in these sample tubes.

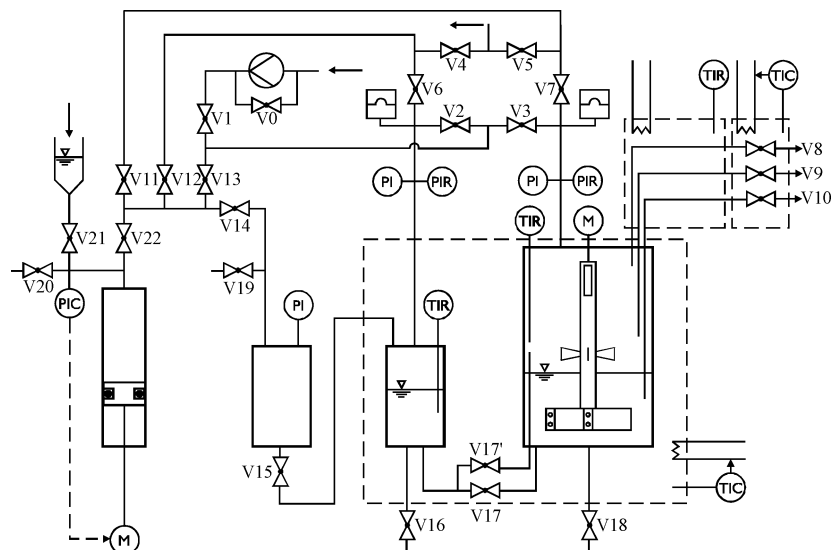


Figure 2. Schematic diagram of the phase equilibrium apparatus.

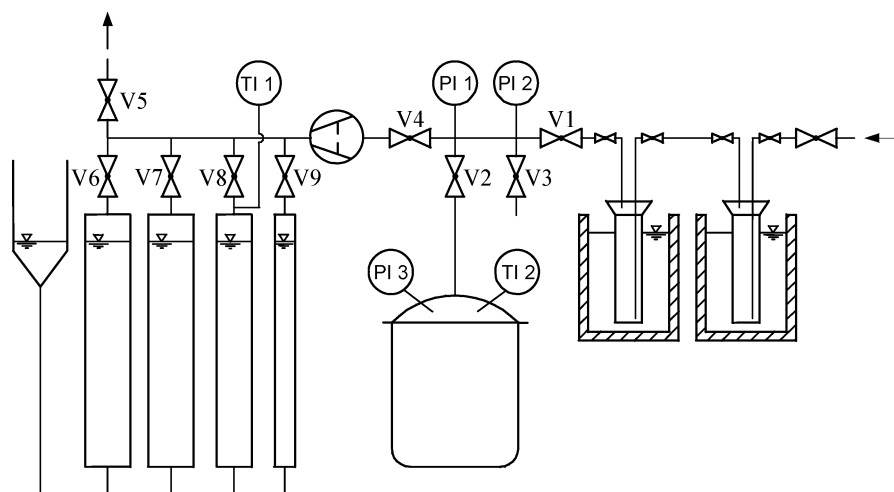


Figure 3. Schematic drawing of the sampling device.

The gaseous part is transferred with a vacuum pump (E2M8HS, Edwards, Sussex, England) into the gas burettes, filled with gas-saturated water. In the case of large amounts of gas, a glass bottle can be used as buffer by opening valve V2 (Figure 3). The amount and composition of the condensable part and the gaseous part are determined, and the composition of the sample is calculated. The procedure is explained in more detail in ref 9.

The samples were analyzed to determine the equilibrium composition of the phases. Sampling of the liquid phase was carried out before sampling of the gaseous phase. The mass was determined by weighing the samples. CO₂ and H₂ passed the sample tubes and were quantitatively determined in the calibrated glass burettes. In the case of mixtures in the liquid and gaseous sample fraction, the composition was determined by gas chromatography (see below).

Accuracy of Measurement. The reliability of the experimental setup used and the experimental procedure applied was verified by comparison to literature data and previously determined equilibrium data, partially using different methods. No systematic errors could be detected within the experimental accuracy, meaning that the deviations were within the errors which occur due to carrying out the measuring procedure. A very detailed discussion of the experimental errors which occur and may be

experienced was carried out by Pfohl.²⁰ Summarizing this discussion, temperatures could be determined to ± 0.1 K for the equilibrium apparatus and ± 0.2 K for the analytical equipment. Pressure was determined with a calibrated bourdon pressure gauge of class 0.6 and a guaranteed accuracy of ± 0.01 MPa. Calibration was regularly repeated with a mechanical pressure balance to an accuracy of ± 10 kPa.

For determination of the composition of the samples, mass could be determined to ± 0.5 mg, gas volume in the burettes to ± 1 %, pressure of the environment to $\pm < 2$ hPa, and concentration by gas chromatography to (1 to 3) %, depending on the type of GC used.

Experimental uncertainties were related to uncertainties in concentration. Concentrations reported are uncertain to (1 to 2) %, which means that for four digits in mole fractions three are quite certain.

3.3. Analysis of the Samples. Further analysis, after separating condensable components from noncondensable ones and determining the sample mass by weighing or by calculating from the gas volume in the burettes, was carried out with gas chromatographic analysis, in the case that more than one compound was present in the samples. From the gaseous and liquid samples of the phase equilibrium measurements, two

Table 3. Phase Equilibrium Data for Squalane–Carbon Dioxide (Mole Fractions)

<i>T</i> [K]	<i>P</i> [MPa]	liquid phase [mol·mol ⁻¹]		gaseous phase [mol·mol ⁻¹]		ref
		<i>x</i> _{Squalane} [-]	<i>x</i> _{CO₂} [-]	<i>y</i> _{Squalane} [-]	<i>y</i> _{CO₂} [-]	
313.15						
313.15	15.00	0.828	0.172	0.9985	0.0015	9
313.15	20.00	0.831	0.169	0.9955	0.0045	9
313.15	25.00	0.843	0.157	0.9959	0.0041	9
313.15	30.00	0.846	0.154	0.9976	0.0024	9
313.15	35.00	0.846	0.154	0.9972	0.0028	9
343.15	15.00	0.797	0.203	0.9995	0.0005	9
343.15	20.00	0.838	0.162	0.9974	0.0026	9
343.15	25.00	0.869	0.131	0.9938	0.0062	9
343.15	30.00	0.878	0.122	0.9925	0.0075	9
343.15	35.00	0.871	0.129	0.9919	0.0081	9
343.15	3.50	0.651	0.349	0.0001	0.9999	13
343.15	5.65	0.495	0.505	0.0001	0.9999	13
343.15	7.20	0.418	0.582	0.0001	0.9999	13
343.15	9.30	0.342	0.658	0.0001	0.9999	13
343.15	10.90	0.295	0.705	0.0001	0.9999	13
343.15	13.10	0.245	0.746	0.0003	0.9997	13
343.15	15.00	—	—	0.0014	0.9986	13
343.15	16.75	0.203	0.707	0.0008	0.9992	13
343.15	19.50	0.206	0.794	0.0023	0.9977	13
343.15	23.60	0.153	0.847	0.0036	0.9964	13
343.15	24.80	0.169	0.831	0.0045	0.9955	13
343.15	28.40	0.124	0.876	0.0066	0.9934	13
343.15	30.10	0.130	0.870	0.0068	0.9932	13
373.7	10.10	0.386	0.614	0.0000	1.0000	13
373.1	13.90	0.306	0.694	0.0001	0.9999	13
373.7	19.60	0.215	0.785	0.0006	0.9994	13
373.7	30.40	0.116	0.884	0.0071	0.9929	13
373.8	30.05	0.120	0.880	—	—	13
423.1	7.90	0.564	0.436	0.0002	0.9998	13
426.0	10.75	0.447	0.523	0.0002	0.9998	13
423.1	14.10	0.377	0.623	0.0003	0.9997	13
422.9	18.00	0.315	0.685	—	—	13
426.0	19.35	0.270	0.730	0.0007	0.9993	13
426.0	30.30	0.144	0.856	0.0050	0.9950	13

Table 4. Phase Equilibrium Data for Squalene–Carbon Dioxide

<i>T</i> [K]	<i>P</i> [MPa]	<i>x</i> _{Sq} [mol·mol ⁻¹]	<i>x</i> _{CO₂} [mol·mol ⁻¹]	<i>y</i> _{Sq} [mol·mol ⁻¹]	<i>y</i> _{CO₂} [mol·mol ⁻¹]	ref
313.15	15.00	0.236	0.764	0.0019	0.9981	10
313.15	20.00	0.225	0.775	0.0030	0.9970	10
333.15	12.00	0.239	0.761	0.0002	0.9998	10
333.15	16.00	0.207	0.793	0.0015	0.9985	10
333.15	20.00	0.186	0.814	0.0029	0.9971	10
333.15	25.00	0.177	0.823	0.0045	0.9955	10
343.15	16.00	0.208	0.792	0.0009	0.9991	10
343.15	20.00	0.190	0.810	0.0021	0.9979	10
343.15	25.00	0.163	0.837	0.0035	0.9965	10
353.15	20.00	0.192	0.808	0.0014	0.9986	10
353.15	23.00	0.174	0.826	0.0026	0.9974	10
353.15	26.00	0.163	0.837	0.0039	0.9961	10
363.15	23.00	0.175	0.825	0.0022	0.9978	10
363.15	26.00	0.165	0.835	0.0035	0.9965	10
363.15	29.50	0.146	0.854	0.0051	0.9949	10
373.15	26.00	0.163	0.837	0.0027	0.9973	10
373.15	29.50	0.147	0.853	0.0042	0.9958	10
333.15	10.00	0.292	0.708	0.0001	0.9999	9
333.15	15.00	0.242	0.758	0.0011	0.9989	9
333.15	20.00	0.200	0.800	0.0014	0.9986	9
333.15	25.00	0.163	0.837	0.0026	0.9974	9
333.15	30.00	0.119	0.881	0.0081	0.9929	9
333.15	35.00	0.103	0.897	0.0104	0.9896	9
363.15	10.00	0.362	0.638	0.0001	0.9999	9
363.15	15.00	0.313	0.687	0.0006	0.9994	9
363.15	20.00	0.229	0.771	0.0013	0.9987	9
363.15	25.00	0.193	0.807	0.0019	0.9981	9
363.15	30.00	0.150	0.850	0.0051	0.9949	9
363.15	35.00	0.083	0.917	0.0134	0.9866	9

samples for analysis were prepared, and each of them was analyzed 2-fold.

The conditions of the gas chromatographic analysis are listed below.

GC-type:	HP 5890 A with FID and Autosampler 7673 A, Hewlett-Packard.
Detector:	FID, <i>T</i> _{FID} = 633 K.
Injection:	“Split/Splitless” capillary-injection system, <i>T</i> _{inj.} = 553 K; equilibration time between injections: 120 s.
Column:	DB-5, length, 30 m; inner diameter, 250 μm; J+W Scientific, Cologne, Germany.
Temperature program:	403 K, 120 s to 473 K, 10 K/60 s. 473 K, 540 s to 563 K, 5 K/60 s. 563 K, 900 s.
Mobile phase:	Nitrogen.
Integrator:	HP 3396-II, Hewlett-Packard, calculating peak area only.

For the analysis of the components squalene and squalane, no internal standard was necessary since only the ratio of the both components had to be determined, which was assumed to be independent of injected quantity.

For the analysis of the gas mixtures of CO₂ and H₂ retrieved from the samples of the phase equilibrium measurements, a gas chromatograph with a packed column was applied. The type and the conditions are listed below.

GC-type:	GC-8APT, Shimadzu.
Detector:	TCD, <i>I</i> = 60 mA.
Injection:	Manually.
Column:	1/8 in.; length, 2 m; inner diameter, 2 mm; prepared in our laboratory using porapak Q (polydivinyl benzene).
Temperature:	303 K.
Mobile phase:	Helium.
Integrator:	Chromatopac C-R2AX, Shimadzu, calculating peak area only.

This method is only able to detect CO₂ with sufficient accuracy since the thermal conductivity of hydrogen and helium are very similar. The gas mixture was injected manually into a sample loop of constant volume. The loop is flushed with the mobile phase which transports the sample onto the column. To avoid deviations, before and after each analysis pure carbon dioxide was injected as a reference for the CO₂ peak area.

3.4. Experimental Results. Phase equilibrium data obtained in our group are listed below for the various systems of the mixture squalane, squalene, hydrogen, and carbon dioxide.

3.4.1. CO₂–Squalane. Experimental values for the system CO₂–squalane, determined for this investigation in our laboratory,^{9,13} are listed in Table 3.

3.4.2. CO₂–Squalene. Our own measurements^{9,10} have been carried out to extend data from the literature and help to verify the method of measurement. These data are listed in Table 4.

Mutual solubility data for the binary system squalene–carbon dioxide are shown in Figure 4 for temperatures of (333 to 373) K and pressures of (12 to 30) MPa. In the gaseous phase, the concentration of squalene raises with pressure at constant temperature. The concentration of squalene in the gaseous phase decreases with increasing temperature at constant pressure since decreasing density induces a reduced solvent power for carbon dioxide which is overriding the increase in volatility with temperature. At conditions equivalent to processing conditions, i.e., 23 MPa and 353 K or 26 MPa and 363 K, the concentration of squalene in the gaseous phase is (2.4 and 3.2) wt %, respectively. In the liquid phase concentration of carbon dioxide also increases with pressure. Temperature is of minor influence.

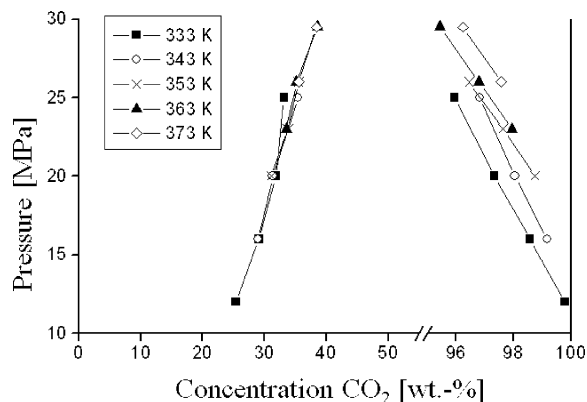
Figure 4. Phase equilibrium for squalene-CO₂.

Table 5. Equilibrium Solubility of Hydrogen in Squalane

T [K]	P [MPa]	x_{Sq} [mol·mol ⁻¹]	x_{H_2} [mol·mol ⁻¹]	ref
327.35	87.20	0.4925	0.5075	13
327.35	30.80	0.6985	0.3015	13
344.15	62.30	0.5320	0.4680	13
344.15	50.20	0.5855	0.4145	13
344.15	30.50	0.6865	0.3145	13
375.05	24.50	0.7080	0.2920	13
375.05	50.80	0.5465	0.4535	13
423.65	81.20	0.3795	0.6205	13
423.65	51.00	0.4880	0.5120	13
423.65	30.40	0.6115	0.3885	13

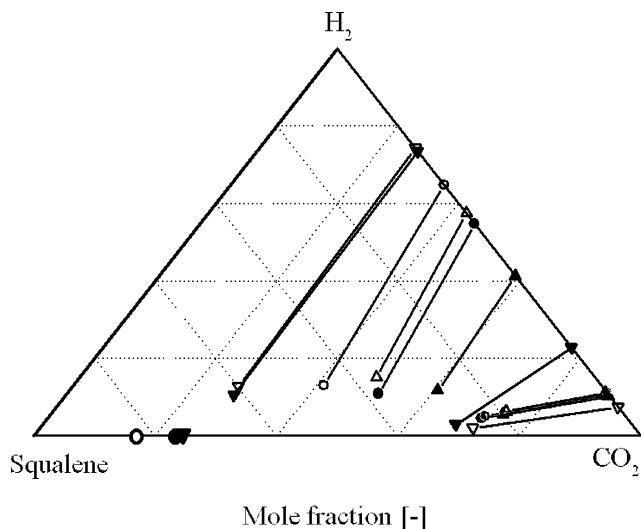
Table 6. Phase Equilibrium Data for the System CO₂-H₂-Squalene (Mole Fractions)

T [K]	P [MPa]	x_{squalene} [-]	x_{CO_2} [-]	x_{H_2} [-]	y_{squalene} [-]	y_{CO_2} [-]	y_{H_2} [-]	ref
310.15	15.00	0.6175	0.2764	0.1061	0.0000	0.2651	0.7349	9
310.15	25.00	0.3768	0.5133	0.1099	0.0000	0.4529	0.5471	9
310.15	35.00	0.2758	0.6065	0.1177	0.0000	0.5870	0.4130	9
310.15	15.00	0.2898	0.6806	0.0296	0.0000	0.7722	0.2278	9
310.15	25.00	0.2389	0.7138	0.0473	0.0009	0.8901	0.1090	9
310.15	35.00	0.1994	0.7455	0.0551	0.0023	0.8947	0.1030	9
330.15	15.00	0.3890	0.5433	0.0677	0.0000	0.5040	0.4960	9
330.15	20.00	0.3708	0.5462	0.0830	0.0000	0.5040	0.4960	9
330.15	25.00	0.3462	0.5674	0.0864	0.0000	0.5250	0.4750	9
330.15	30.00	0.3223	0.5702	0.1075	0.0000	0.5383	0.4617	9
330.15	35.00	0.3058	0.5653	0.1289	0.0000	0.5340	0.4660	9
330.15	15.00	0.2930	0.6737	0.0333	0.0001	0.7608	0.2391	9
330.15	20.00	0.2735	0.6845	0.0420	0.0000	0.8156	0.1844	9
330.15	25.00	0.2374	0.7112	0.0514	0.0002	0.8387	0.1611	9
330.15	30.00	0.2163	0.7248	0.0589	0.0006	0.8569	0.1425	9
330.15	35.00	0.2021	0.7292	0.0687	0.0010	0.8425	0.1565	9
330.15	15.00	0.6155	0.2760	0.1085	0.0000	0.2541	0.7459	9
330.15	20.00	0.5116	0.3758	0.1126	0.0000	0.3004	0.6996	9
330.15	25.00	0.4870	0.3953	0.1177	0.0000	0.3348	0.6652	9
330.15	30.00	0.4871	0.3595	0.1534	0.0000	0.3001	0.6999	9
330.15	35.00	0.4970	0.3064	0.1966	0.0000	0.2617	0.7383	9
350.15	15.00	0.2662	0.7134	0.0204	0.0000	0.9252	0.0748	9
350.15	25.00	0.2315	0.7175	0.0510	0.0019	0.8876	0.1119	9
350.15	35.00	0.1898	0.7467	0.0635	0.0017	0.8862	0.1121	9
350.15	15.00	0.5984	0.2729	0.1287	0.0000	0.2575	0.7425	9
350.15	25.00	0.4562	0.4116	0.1322	0.0000	0.3522	0.6478	9
350.15	35.00	0.3596	0.4897	0.1507	0.0000	0.4261	0.5739	9

The two-phase area of the binary system extends beyond the 30 MPa to which measurements were limited.

3.4.3. Squalane-Hydrogen. For squalane-hydrogen, only the solubility of hydrogen in the liquid phase was determined (Table 5)¹³ since at the time of the measurement of the data there was interest only in the composition of the liquid phase. Equilibrium solubility data were used in connection with measuring diffusion coefficients for which the equilibrium value provides the driving potential.

3.4.4. CO₂-H₂-Squalene and CO₂-H₂-Squalane. Phase equilibrium data for the ternary system CO₂-H₂-squalene as

Figure 5. Phase equilibrium data for CO₂-H₂-squalene at 310 K (full symbols) and 350 K (open symbols). ▽/▽, 15 MPa; ●/○, 20 MPa; ▲/△, 25 MPa.Table 7. Phase Equilibrium Data for the System CO₂-H₂-Squalene (Mole Fractions)

T [K]	P [MPa]	x_{squalene} [-]	x_{CO_2} [-]	x_{H_2} [-]	y_{squalene} [-]	y_{CO_2} [-]	y_{H_2} [-]	ref
343.15	31.80	0.447	0.327	0.226	0.0000	0.2010	0.7990	13
343.15	57.40	0.397	0.229	0.374	0.0000	0.1470	0.8530	13
343.15	55.30	0.382	0.286	0.332	0.0000	0.1250	0.8750	13
343.15	30.40	0.286	0.538	0.176	0.0002	0.5569	0.4429	13
343.15	65.20	0.261	0.472	0.267	0.0000	0.4160	0.5840	13
343.15	65.10	0.150	0.539	0.311	0.0024	0.3432	0.6544	13
373.15	67.90	0.263	0.371	0.366	0.0000	0.3120	0.6880	13
423.15	49.50	0.329	0.356	0.315	0.0001	0.3109	0.6890	13
423.15	66.50	0.293	0.322	0.385	0.0001	0.2280	0.7719	13

determined in our laboratory⁹ are listed in Table 6 for temperatures of (310, 330, and 350) K. At (310 and 350) K two different concentration ranges were determined at pressures of (15, 25, and 35) MPa. Data are shown in Figure 5. Phase equilibrium data for the ternary system CO₂-H₂-squalene as determined in our laboratory¹³ are listed in Table 7 for temperatures of (343, 373, and 423) K.

The distance between the individual experimental points is relatively great. To be able to interpolate, at 330 K, three different concentration ranges at pressures of (15, 20, 25, 30, and 35) MPa were investigated. Interpolation is to be carried out by modeling the equilibrium data with equations of state. In this work, the Soave-Redlich-Kwong equation of state was chosen, as will be discussed in more detail below. Missing intermediate values can be created by this method with good accuracy. For the data at 330 K, the modeling procedure will be demonstrated below.

3.4.5. Squalene-Squalane-CO₂-H₂. The quaternary system squalene-squalane-CO₂-H₂ was investigated in our laboratory⁹ at the same temperatures as the ternary system squalene-CO₂-H₂, i.e., (310, 330, and 350) K. Results are listed in Table 8. If the very similar compounds squalene and squalane are lumped into one pseudocomponent, the phase behavior of the quasi-ternary system is very similar to the ternary system shown in Figure 6. Therefore, the quaternary system was not investigated in detail. Measurements were only carried out at pressures of (15, 25, and 35) MPa and for two concentration ranges.

Table 8. Phase Equilibrium Data for the Quaternary System CO₂–H₂–Squalane–Squalene (Mole Fractions)

<i>T</i> [K]	<i>P</i> [MPa]	<i>x</i> _{CO₂} [-]	<i>x</i> _{H₂} [-]	<i>x</i> _{Squalene} [-]	<i>x</i> _{Squalane} [-]	<i>y</i> _{CO₂} [-]	<i>y</i> _{H₂} [-]	<i>y</i> _{Squalene} [-]	<i>y</i> _{Squalane} [-]	ref
310.15	15.00	0.3484	0.0489	0.3155	0.2872	0.3616	0.6384	0.0000	0.0000	9
310.15	25.00	0.5895	0.1005	0.1624	0.1476	0.4520	0.5480	0.0000	0.0000	9
310.15	35.00	0.5869	0.1350	0.1460	0.1321	0.4892	0.5108	0.0000	0.0000	9
310.15	15.00	0.7193	0.0307	0.1316	0.1184	0.8631	0.1369	0.0000	0.0000	9
310.15	25.00	0.7361	0.0651	0.1048	0.0940	0.8787	0.1193	0.0010	0.0010	9
310.15	35.00	0.7345	0.0762	0.0999	0.0894	0.8790	0.1181	0.0015	0.0014	9
330.15	15.00	0.5198	0.0659	0.2188	0.1955	0.8920	0.1080	0.0000	0.0000	9
330.15	25.00	0.5498	0.1236	0.1729	0.1537	0.9178	0.0791	0.0015	0.0016	9
330.15	35.00	0.8196	0.0451	0.0718	0.0635	0.9170	0.0754	0.0038	0.0038	9
330.15	15.00	0.5596	0.0481	0.2084	0.1839	0.5241	0.4759	0.0000	0.0000	9
330.15	25.00	0.5856	0.0828	0.1762	0.1554	0.4581	0.5419	0.0000	0.0000	9
330.15	35.00	0.6176	0.1218	0.1386	0.1220	0.4640	0.5360	0.0000	0.0000	9
350.15	15.00	0.6987	0.0198	0.1499	0.1316	0.9126	0.0874	0.0000	0.0000	9
350.15	25.00	0.7629	0.0352	0.1075	0.0944	0.9128	0.0861	0.0005	0.0006	9
350.15	35.00	0.7884	0.0554	0.0832	0.0730	0.9188	0.0781	0.0015	0.0016	9
350.15	15.00	0.4378	0.0739	0.2600	0.2283	0.4640	0.5360	0.0000	0.0000	9
350.15	25.00	0.6156	0.0694	0.1679	0.1471	0.5919	0.4081	0.0000	0.0000	9
350.15	35.00	0.7060	0.0796	0.1144	0.1000	0.5916	0.4080	0.0002	0.0002	9

4. Calculation of the System Squalene–Squalane–CO₂–H₂ and the Underlying Binary and Ternary Systems

4.1. Method: Calculation Program PE.²¹ For modeling of phase equilibria, different methods, based on the fundamental equations for equilibrium, have been developed and can be used. The type of model and the specific equations depend on the compounds of the system, in particular, their individual properties and the interactions between alike and different molecules. Also important is the goal to be achieved with the modeling. Screening calculations require less accurate and sophisticated models than design calculations. In consequence, there is no universal model or method available for simulating phase equilibria. The result of the calculations strongly depends on the type selected and on the knowledge and dedication of the user.

Modeling of phase equilibria at higher pressures and in systems containing not too many compounds is mostly achieved with equations of state (EOS) and mixing rules. The bases are binary systems, which are combined to multicomponent systems. In this work, components in the supercritical state, H₂ and CO₂, together with hydrocarbon chain molecules, squalane, and

squalene have to be modeled. All compounds are nonpolar or at highest slightly polar. Modeling of phase equilibrium of these compounds can be anticipated to be successfully possible with cubic equations of state. From these, the Soave–Redlich–Kwong (SRK) modification of the van der Waals EOS was selected after the first sample calculations. The Peng–Robinson modification often is preferred,²⁰ but it proved in our case less accurate for the prediction of equilibrium data than the SRK-EOS. As a mixing rule, the one published by Mathias et al.²² was used, thus avoiding the Michelsen–Kistenmacher effect.

One of the prerequisites for phase equilibrium calculations are accurate pure component parameters. While they are well-known for low molecular weight compounds, for the compounds squalane and in particular squalene, this is not the case. Therefore, the first task comprised the determination of pure component parameters for the EOS.

4.2. Determination of Pure Component Parameters for the SRK-EOS. Basically, pure component parameters are given by the values for the critical constants, *T_C*, *P_C*, and the acentric factor *ω*. These values are not available for squalene and squalane. For such compounds, it is advisable not to use predictive methods for the critical values but to consider the parameter of the EOS as adjustable parameters and fit them to experimental data. These can be chosen in a region of temperature and pressure, if possible, similar to that region of *P* and *T* for which the equilibrium calculations will be carried out. Although this procedure may be considered theoretically not attractive, in practice it is very effective. Other methods may lead to unacceptable values for the fitted parameter, e.g., for interaction coefficients.

For carbon dioxide and hydrogen, the parameters for the SRK-EOS are published in the literature, e.g., refs 23 and 24. To be consistent in our calculation scheme, these parameters were also derived from fitting data to the SRK-EOS. The procedure is explained in the following. Data for *T_C*, *P_C*, and *ω* are compiled in Table 2.

For squalane, vapor pressure data have been measured and published by Mokbel et al.²⁵ and were used for calculating the pure component parameter. In addition, vapor pressures for squalane had been determined by molecular simulation by Neubauer et al.,²⁶ which enabled a comparison of the results of our correlation at higher temperatures also. This correlation was carried out with our program system PE.²¹

Parameters of the EOS can be chosen such that correlated data represent the experimental data with highest accuracy. Data

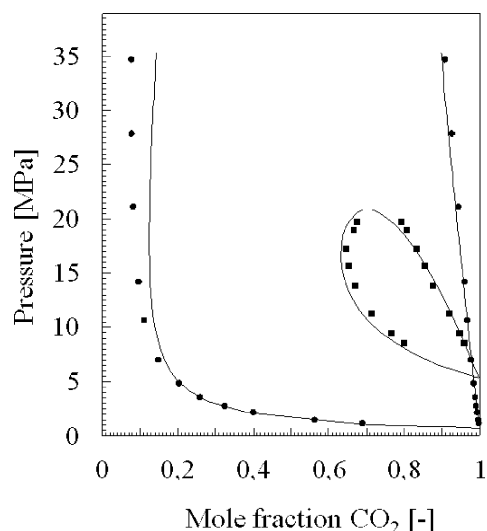


Figure 6. *P*, *x* diagram of the binary system CO₂–H₂. Experimental data: Tsang and Streett.¹¹ ●, 225 K; ■, 290 K; — correlation with SRK-EOS, MKP mixing rule. Parameter (component 1: CO₂): *k*₁ = 0.0989; *l*₁ = 0; *λ*₁₂ = –0.2499.

Table 9. Pure Component Parameters As Calculated with the SRK-EOS

component	T_C [K]	P_C [MPa]	ω [-]
hydrogen	33.67	1.27	-0.2738
carbon dioxide	310.11	8.28	0.1940
squalane	822.89	1.13	1.1515
squalene	782.13	1.11	1.9083

for correlating the pure component parameters were liquid densities at saturation conditions and vapor pressures.^{20,27}

Table 9 lists the pure component parameters as calculated with the SRK-EOS using the above-described methods. These parameters were applied for calculation of the phase equilibria of this work.

It is obvious that the calculated values for the critical point of carbon dioxide are higher than the real ones. Calculations in the near critical region of CO₂ may thus lead to errors. The range of conditions of interest for hydrogenation—which is the background for the phase equilibrium calculations—($P > 10$ MPa, $T > 313.15$ K) is far from that critical point. Therefore, the deviations will not be of influence.

Furthermore, high values of the acentric factor ω for squalane and squalene are correlated. In such cases, cubic EOS are usually not applied for modeling the properties of pure components. It is assumed that eicosane (C₂₀H₄₂), molecular weight of 282.6 g·mol⁻¹ with an acentric factor of 0.91, represents the limit for correlations with cubic EOS. Because of the calculated high critical temperatures for squalane and squalene, the phase equilibrium calculations are carried out at low reduced temperatures ($T_r < 0.5$). Since most thermodynamic information which has been used for developing cubic EOS is in the range of $T_r > 0.5$, it is assumed that the correlation should not be sufficiently accurate in this region. The successful correlations of this work prove on the other hand that this conclusion cannot be generalized, in particular, not for systems with small molecular interaction forces.

4.3. System CO₂-H₂. Phase equilibria of the system CO₂-H₂ have been determined experimentally by Tsang and Streett¹¹ for temperatures of (220 to 290) K and for pressures up to 172 MPa. In Figure 6 the correlation results for two temperatures, (225 and 290) K, are shown for that system, using the Soave-Redlich-Kwong equation of state (SRK-EOS) and the Mathias-Klotz-Prausnitz (MKP) mixing rule.

One set of interaction parameters k_{12} and λ_{12} is sufficient to correlate the equilibrium data for that temperature range with sufficient accuracy. The interaction parameter l_{12} can be set to zero. At temperatures higher than about 295 K, the system is totally miscible and consists of one phase. Since this temperature is far below the temperature range for hydrogenation, (310 to 330) K, total miscibility can be assumed for hydrogen and carbon dioxide throughout the hydrogenation.

4.4. Binary Systems H₂-Squalane and H₂-Squalene. Phase equilibrium data for the system H₂-squalane had been determined by Brunner¹³ and Löhrl-Thiel¹⁴ in connection with the measurement of diffusion coefficients. Figure 7 presents the phase equilibrium for temperatures of (327.15 and 344.15) K and the correlated data.

The two-phase area in this system extends to very high pressures. Solubility of squalane in hydrogen is very low, even at high pressures up to about 90 MPa. The low mutual solubility of the components is due to the low interaction forces between molecules, which results in low interaction coefficients k_{12} and λ_{12} for the MKP mixing rule.

For the system H₂-squalene, no phase equilibrium data had been found in the literature. Since squalene and squalane only

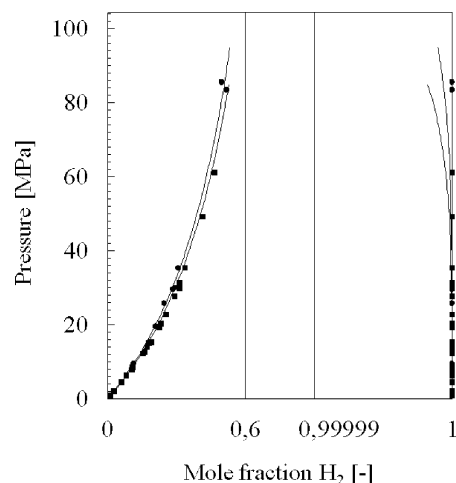


Figure 7. P, x diagram for the binary system H₂-squalane. ●, 327.15 K; ■, 344.15 K;^{13,14} —, correlation with SRK-EOS, MKP mixing rule. Parameter (component 1: H₂): $k_{12} = -0.0486$; $l_{12} = 0$; $\lambda_{12} = 0.0794$.

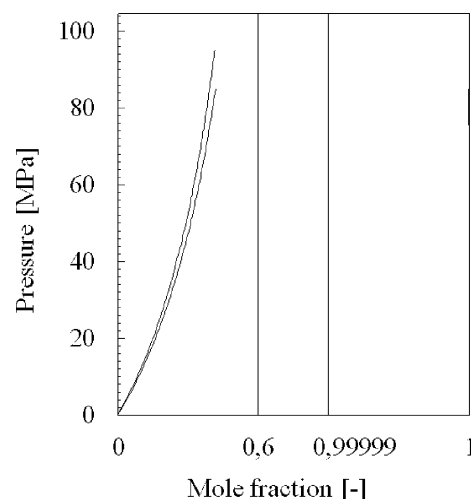


Figure 8. P, x diagram for the binary system H₂-squalene. ●, 327.15 K; ■, 344.15 K; —, correlation with SRK-EOS, MKP mixing rule. Parameter (component 1: H₂): $k_{12} = -0.0486$; $l_{12} = 0$; $\lambda_{12} = 0.0794$.

differ by the double bonds of squalene, a very similar phase behavior in connection with hydrogen is assumed. The interaction parameter derived from the system H₂-squalene was also used for H₂-squalene. Deviations in the calculated phase behavior are therefore related to the different values for T_C , P_C , and ω . The calculated phase equilibrium data for H₂-squalene are very similar to that of H₂-squalane (Figure 8). The mutual solubility is even lower, due to the higher acentric factor for squalene. Solubility of squalene in hydrogen is very low.

4.5. Binary Systems CO₂-Squalane and CO₂-Squalene. Phase equilibrium data for the system CO₂-squalane were measured by Liphard and Schneider¹² and later by Brunner¹³ and Löhrl-Thiel.¹⁴ Data determined for this work are in good coincidence with the literature data. Therefore, data were only measured for the lower temperature of 313.15 K. In Figure 9, data and correlations are shown for (313.15, 343.15, and 373.15) K and for pressures up to 35 MPa. The two-phase region extends to high pressures. The correlation with the SRK-EOS and the MKP mixing rule confirms this and even predicts for the lower temperatures an open-phase diagram, corresponding to a type III phase behavior. At the higher temperature, the two-phase area closes in the region of about 70 MPa as experimental data from Liphard and Schneider show. According to their data, the

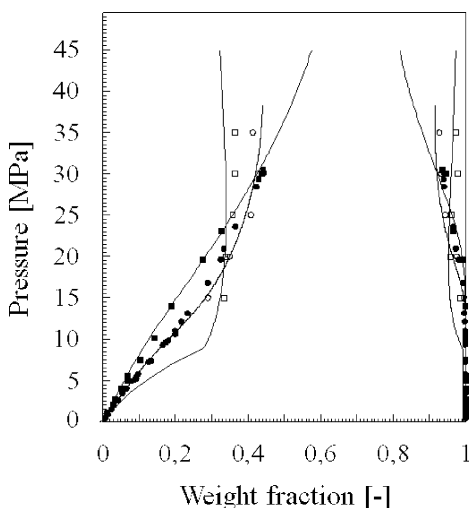


Figure 9. P,x diagram for the binary system CO_2 -squalane. ●, 343.15 K; ■, 373.15 K.^{12,13} Own measurements: □, 313.15 K; ○, 343.15 K; —, correlation with SRK-EOS, MKP mixing rule. Parameter (component 1: CO_2): $k_{12} = 0.0176$; $l_{12} = 0$; $\lambda_{12} = -0.1133$.

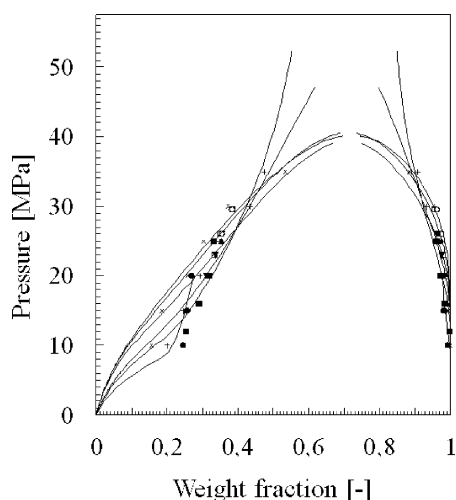


Figure 10. P,x diagram of the binary system CO_2 -squalene. ●, 313.15 K; ■, 333.15 K; ▲, 343.15 K; ▼, 353.15 K; □, 363.15 K; ○, 373.15 K.⁶ Own measurements: +, 333.15 K; ×, 363.15 K; —, correlations with SRK-EOS and MKP mixing rule. Parameters: see Table 10.

Table 10. Parameter for the MKP Mixing Rule for Modeling the System CO_2 -Squalene with the SRK-EOS (Component 1: CO_2)

T [K]	k_{12} [-]	λ_{12} [-]	l_{12} [-]
313	0.1071	0.0748	0
333	0.1035	0.0864	0
343	0.0986	0.0792	0
353	0.1398	0.1592	0
363	0.1346	0.1485	0
373	0.1181	0.1220	0

two-phase area closes at 328.15 K and 70.5 MPa with decreasing tendency for the maximum pressure with increasing temperature leading to a full miscibility at 373.15 K and 36.3 MPa. Up to pressures of about 35 MPa in a temperature range of (313.15 to 373.15) K, correlation of the experimental data is in good coincidence with experimental values, using only one data set of parameter k_{12} and λ_{12} ; l_{12} can be set to zero.

Phase equilibrium data for the system CO_2 -squalene had been determined by Saure.¹⁰ Figure 10 shows the P,x diagram for temperatures of (313.15 to 373.15) K at pressures up to 35 MPa. Our own measurements are in good coincidence with these data. Therefore, no additional data were determined.

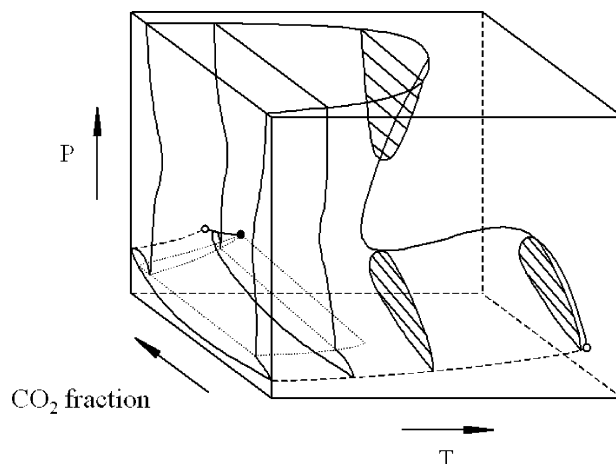


Figure 11. Schematic representation of the phase behavior of the binary systems CO_2 -squalane and CO_2 -squalene (type III).

Table 11. Minimum Values for the Critical Curves for the Binary Systems CO_2 -Squalane and CO_2 -Squalene

system	temperature minimum	pressure minimum
CO_2 -squalane	328 K; 70.5 MPa	373 K; 36.3 MPa
CO_2 -squalene	340 K; 55 MPa	370 K; 38 MPa

According to our calculations, the two-phase area closes for this system also only at temperatures above about 340 K in a pressure range of (38 to 55) MPa. The maximum pressure for two phases (the critical pressure for the binary system) is decreasing to 38 MPa with increasing temperature and then again increasing. The schematic phase behavior is shown in Figure 11, corresponding to a type III behavior. Correlation of phase equilibrium data is good for the temperature range from (313.15 to 373.15) K up to pressures of 35 MPa. The interaction parameter for this system proved to be temperature dependent. For each correlation temperature, a separate set of parameters for k_{12} and λ_{12} of the MKP mixing rule had to be applied, as shown in Table 10.

For the understanding of the phase behaviors of the systems CO_2 -squalane and CO_2 -squalene, a generalized diagram is shown in Figure 11, representing the type III phase behavior, which can be assumed for that type of system. The critical curve is divided into two legs. One leg begins at the critical point of the component of lower volatility (squalene, squalene). With decreasing temperature, the critical pressures increase up to a maximum value, decrease to a minimum with further decreasing temperature, and then rapidly increase to very high pressures without coming back into the critical region of the component of higher volatility (CO_2), running through a temperature minimum for the one-phase area.

The minimum values and the corresponding pressures are listed in Table 11 for both systems. Values for CO_2 -squalane are based on data of Liphard and Schneider,¹² and those for CO_2 -squalene stem from the correlations with the SRK-EOS. The second leg of the critical curve begins at the critical point of the component of higher volatility (CO_2) and ends in a critical end-point of the three-phase line liquid-liquid-gas.

4.6. Ternary Systems CO_2 - H_2 -Squalane and CO_2 - H_2 -Squalene. The correlation of the ternary systems is carried out with the interaction parameter of the binary subsystems, determined at the same temperature, without further fitting to experimental data. In Figure 12, these correlations are shown for the system CO_2 - H_2 -squalane at $T = 343.15$ K and $P = (31.8, 35, \text{ and } 55.3)$ MPa and at $T = 373.15$ K and $P = 67.9$ MPa. Comparison of the correlated data to experimental values

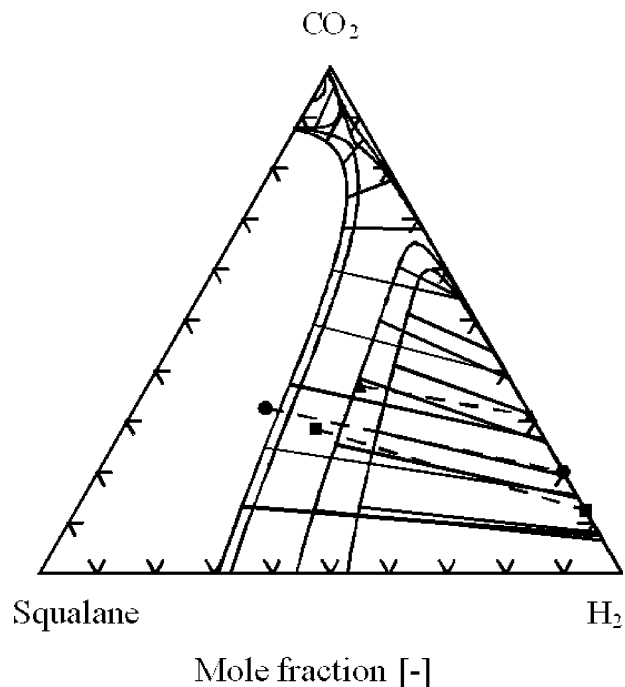


Figure 12. Phase equilibrium for the ternary system CO₂-H₂-squalane. $T = 343.15$ K: ●, 31.8 MPa; ■, 55.3 MPa. $T = 373.15$ K: ▲, 67.9 MPa;²⁰ —, correlation with the SRK-EOS and the MKP-mixing rule.

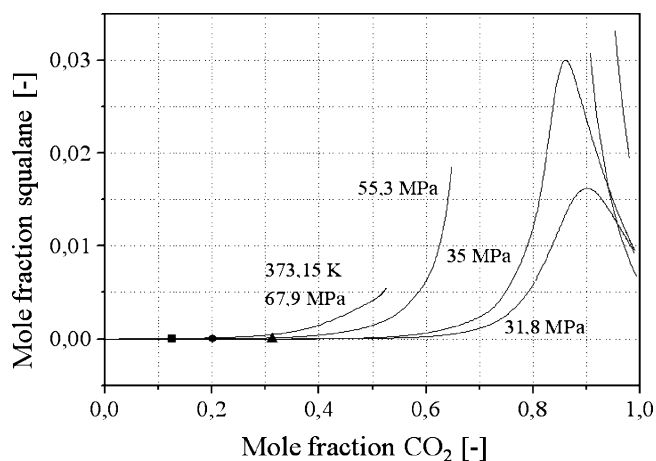


Figure 13. Enlarged representation of the gaseous phase of the ternary system CO₂-H₂-squalane at 343.15 K (●, 31.8 MPa; ■, 55.3 MPa; and 373.15 K; ▲, 67.9 MPa).

determined by Brunner¹³ revealed a good coincidence. Only at 373.15 K and 67.9 MPa deviations are somewhat higher. This may be due to the fact that experiments with the ternary systems were carried out at much higher pressures than the pressures at which the interaction parameter for the binary system CO₂-squalane were determined. Therefore, deviations occur at high pressures. Inclination of the connodes is correctly represented in all cases.

Simulation of the phase equilibrium reveals that the two-phase area is narrowing down with increasing pressure. In the temperature range, where the subsystem CO₂-squalane shows an open two-phase area with respect to pressure, the two-phase area in the ternary system is showing a pinch which results in two separate two-phase areas with increasing pressure (see Figure 12 near the upper triangle point representing CO₂).

Experimental data and calculated connodes are not clearly seen for the gaseous phase. Therefore, the gaseous phase is enlarged in Figure 13. Now, the influence of the hydrogen

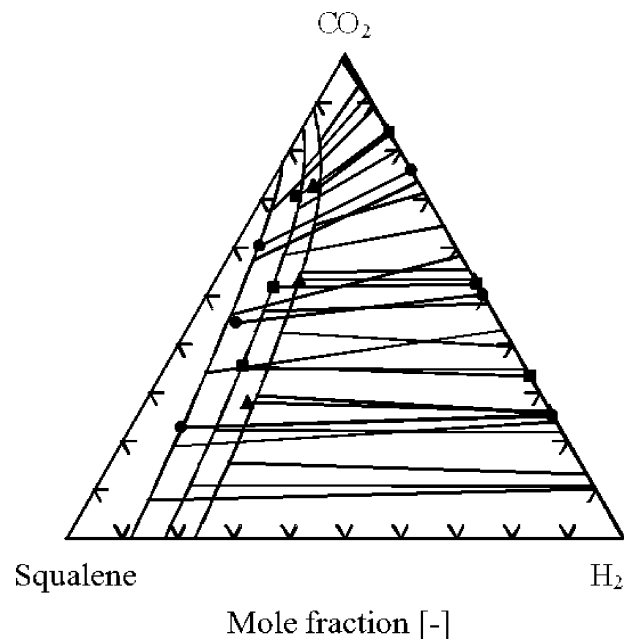


Figure 14. Experimental and calculated phase equilibrium data for the system CO₂-H₂-squalane at $T = 330$ K. ●, 15 MPa; ■, 25 MPa; ▲, 35 MPa. Lines are calculated with the SRK-EOS using the MKP (Mathias-Klotz-Prausnitz) mixing rule.

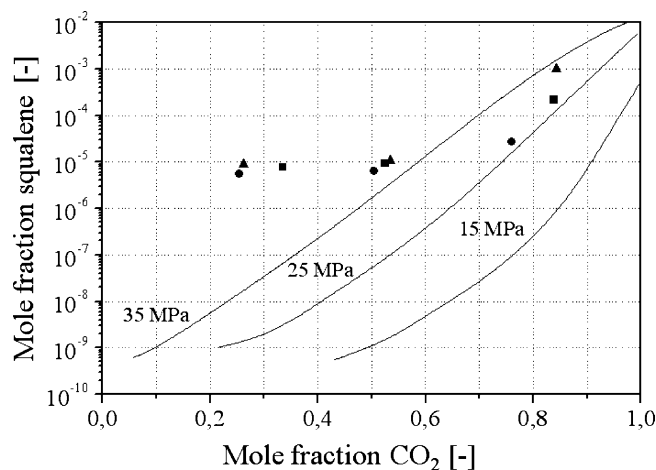


Figure 15. Enlarged representation of the gaseous phase for the ternary system CO₂-H₂-squalane at 330 K. ●, 15 MPa; ■, 25 MPa; ▲, 35 MPa.

concentration on the solubility of squalane in the gaseous phase and the connodes connecting the equilibrium phases are made clear. Squalane is nearly nonsoluble in the gaseous phase at high concentrations of hydrogen, as found also experimentally. At hydrogen concentrations below 0.5 mol·mol⁻¹, solubility of squalane in the gaseous phase increases rapidly. Phase boundary lines show a maximum for concentrations of 0.6 to 0.9 of CO₂ or full miscibility.

Correlation of the phase equilibrium for the system CO₂-H₂-squalane at a temperature of 330 K and pressures of (15, 25, and 35) MPa is shown in Figure 14. Correlation was carried out using the SRK-EOS. Correlated data and experimental data, as well as connodes, are in good coincidence. The gaseous phase is shown enlarged in Figure 15.

The two-phase area shrinks with increasing pressure. Due to lacking data, representation was limited to 35 MPa. The binary subsystem CO₂-squalane at temperatures below 343 K also has a two-phase area which extends beyond that pressure. Therefore,

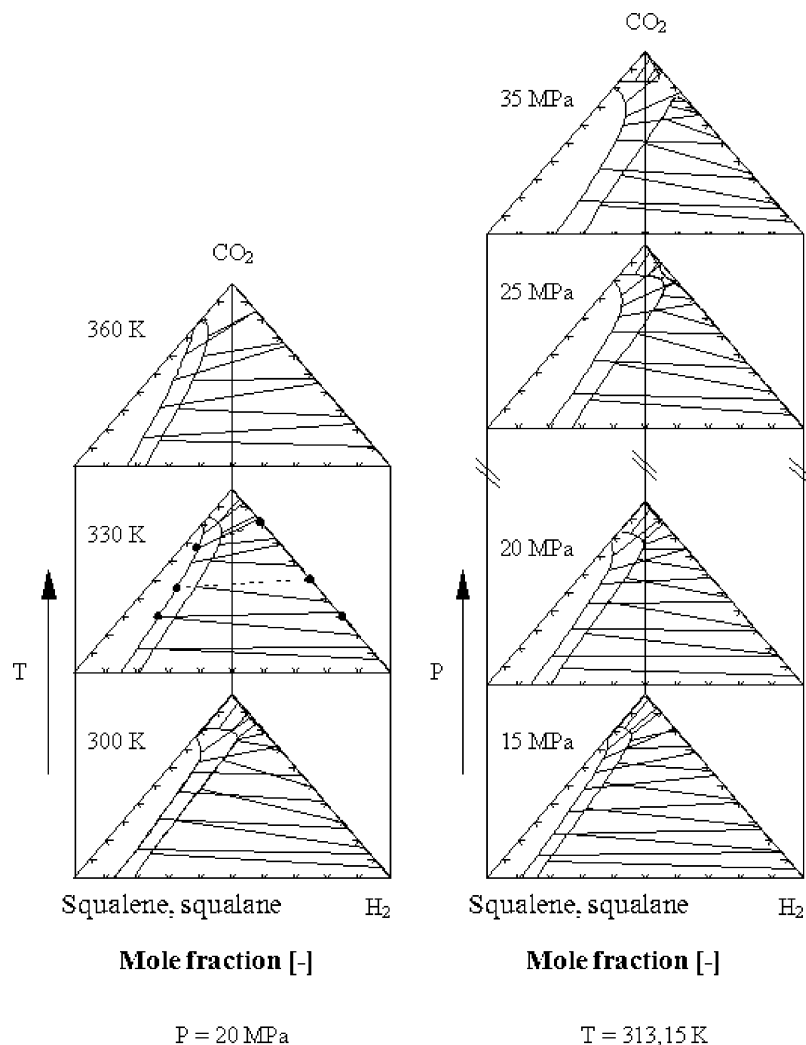


Figure 16. Representation of the ternary systems $\text{CO}_2\text{-H}_2\text{-squalane}$ and $\text{CO}_2\text{-H}_2\text{-squalene}$ in dependence on temperature (left side) and on pressure (right side).

also in the ternary system $\text{CO}_2\text{-H}_2\text{-squalene}$, a shrinking of the two-phase area can be anticipated at higher pressures. Calculated results for a temperature of 330 K predict a splitting into separate areas of two-phase equilibrium at a pressure of 58.5 MPa.

An enlarged representation of the gaseous phase is necessary also for this system to see the quality of the calculations with respect to the equilibrium in the gaseous phase. Calculated solubility for squalene in mixtures of hydrogen and carbon dioxide is much smaller than the values determined experimentally. Therefore, in Figure 15, a logarithmic scale was used. The calculated binodal curves lie optically far off the experimental data. The reason is high relative errors, which is plausible due to the very small numbers in the order of 10^{-5} , resulting in small absolute errors.

The solubility of squalene drops rapidly with increasing concentration of hydrogen, as is the case for squalane. During a hydrogenation reaction, a phase splitting may occur if hydrogen is added to the mixture of carbon dioxide–squalene. In any case, an enlarged two-phase area will be formed. In the pressure range shown here, the phase boundary lines (binodal curves) exhibit no maximum since the two-phase area is not shrinking at that pressure level. Yet, the points of inclination in the range of 0.8 indicate already that at higher pressures a similar phase behavior will occur.

Temperature and pressure dependence of the ternary phase equilibrium is illustrated in Figure 16.

4.7. Quaternary System $\text{CO}_2\text{-H}_2\text{-Squalane-Squalene}$. Representation of quaternary systems in diagrams is difficult. Therefore, the components squalane and squalene are lumped in a pseudocomponent. All experimental data for the ternary systems showed that the ratio of concentrations of squalene and squalane in the gaseous and the liquid phases is very near to one and that the phase equilibrium for the ternary systems is very similar. This makes it possible to represent the quaternary system as a pseudoternary system using Gibbs diagrams without losing much information. All calculations have been carried out for the quaternary system and are only graphically presented as pseudoternary data.

In Figure 17, the temperature and pressure dependence of phase equilibria of the pseudoternary system is shown in separate prisms for a pressure of 250 bar and temperatures of (310, 330, and 350) K and at a temperature of 330 K and pressures of (15, 25, and 35) MPa. Experimental data are shown for the quaternary system and the results obtained with the SRK-EOS modeling for the subsystems. For better orientation in both diagrams, correlated and experimental data for the ternary systems are also included.

Experimental and correlated data are in good coincidence. In particular, the inclination of the connodes is very well represented. The connodes lie in between the binodal curves of the ternary

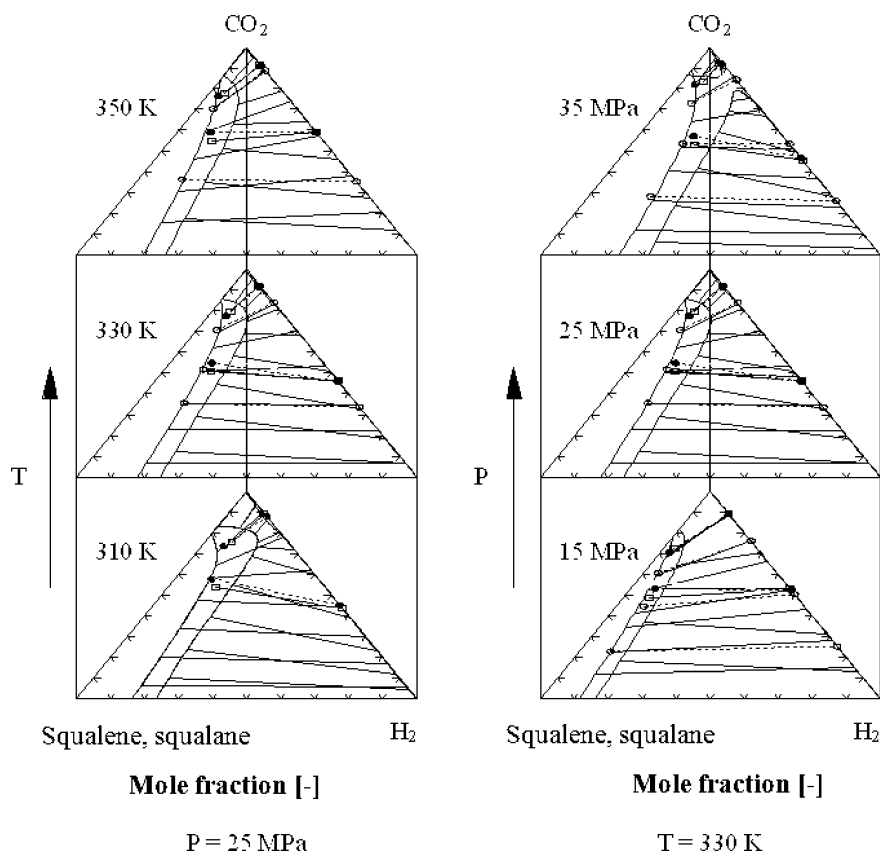


Figure 17. Phase behavior of the quaternary system $\text{CO}_2\text{-H}_2\text{-squalene-squalene}$ in a pseudoternary representation. Left hand side: temperature dependence. Right-hand side: pressure dependence. ●, experimental data points; □, calculated with SRK-EOS; ○, experimental data points of the ternary systems $\text{CO}_2\text{-H}_2\text{-squalene}$ (for comparison). Inner two-phase area, ternary system $\text{CO}_2\text{-H}_2\text{-squalene}$ (for comparison); outer two-phase area, ternary system $\text{CO}_2\text{-H}_2\text{-squalene}$ (for comparison).

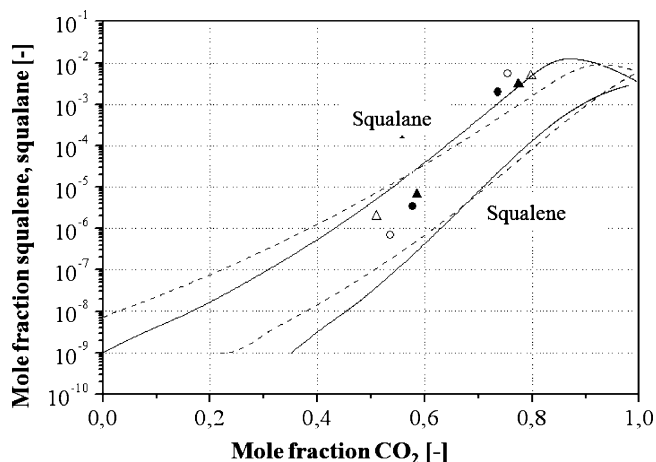


Figure 18. Enlarged representation of the gaseous phase of the quaternary system $\text{CO}_2\text{-H}_2\text{-squalene-squalene}$ at (310 and 330) K at 25 MPa. Full lines, 310 K; broken lines, 330 K. ●/○, calculated/experimental data for the pseudocomponent squalene + squalene at 313.15 K; ▲/△, calculated/experimental data for the pseudocomponent squalene + squalene at 373.15 K.

subsystems. This confirms the assumption that the interaction of the components squalane and squalene is relatively small and of such a character that it does not influence the phase behavior. The binary interaction coefficients are therefore set to zero in the MKP mixing rule. Both components can be represented by a pseudocomponent with a solubility in the mixture of carbon dioxide and hydrogen between that of the two pure components. Inclination of the connodes behaves similarly.

An interesting difference between the experimental results and the calculated values is that the experimentally determined solubility always is somewhat lower than the calculated solubility. On the contrary, the experimentally determined solubility for the components squalane and squalene has been always higher than the calculated ones. In Figure 18, experimental data points for the liquid phase are shifted to the binodal curves of the ternary subsystems $\text{CO}_2\text{-H}_2\text{-squalene}$ or are lying on the binodal curve. At $T = 330$ K and $P = 35$ MPa, this behavior is especially pronounced. The calculation predicts at a concentration of 80 % CO_2 complete miscibility of the ternary subsystem $\text{CO}_2\text{-H}_2\text{-squalene}$, but experimental data do not give any hint in this direction. Two phases are coexisting, and the ratio of the concentrations of squalane and squalene is close to one in both phases. This indicates that the two-phase area exists also in the quaternary system as well as in the system with squalane.

Representation of the gaseous phase has to be shown in a separate diagram because of the different scale needed. In Figure 18, the gaseous phase of the quaternary system is shown for temperatures of (310 and 330) K and a pressure of 25 MPa on a pseudoternary basis. For comparison, the binodal curves of the ternary subsystems $\text{CO}_2\text{-H}_2\text{-squalene}$ and $\text{CO}_2\text{-H}_2\text{-squalene}$ are shown. Experimentally determined and calculated solubility is in good coincidence. For mole fractions of 0.5 to 0.6 for CO_2 , both values are in between the binodal curves of the ternary subsystems. At higher concentrations of CO_2 , experimental and calculated results for the solubility are higher than that for the ternary subsystems. It seems that for the calculation of the ternary subsystems the solubility of the

components squalane and squalene is underestimated. However, it is surprising how accurately the solubility for the quaternary system can be calculated.

5. Conclusion

The results enable planning of a hydrogenation of squalene to squalane using supercritical carbon dioxide as a modifier for solubility in both phases. VLE data were determined for the systems CO₂-H₂-squalene and CO₂-H₂-squalene-squalane in the temperature and pressure ranges of (310 to 350) K and (150 to 350) bar. The quaternary system CO₂-H₂-squalene-squalane and all subsystems can be correlated with cubic equations of state. The authors used the program package *PE*, developed at the department for Thermal and Separation Processes at the Hamburg University of Technology and available on the Internet. On the basis of our own measurements and on literature data, it was possible to correlate and predict the phase behavior in the process relevant range. It is even possible to extrapolate with sufficient accuracy to be able to plan additional measurements, if this is found to be necessary.

Acknowledgment

The advice of Prof. John O'Connell helped with thermodynamic problems. The support of Prof. Dr. G. M. Schneider, especially in the early stages of the experimental work on phase equilibrium determination, is still not forgotten.

Literature Cited

- (1) Brunner, G. *Gas Extraction - An Introduction to Fundamentals of Supercritical Fluids and the Application to Separation Processes*; Steinkopff: Darmstadt, Springer: New York, 1994.
- (2) Römpf, *Lexikon Chemie*; Georg Thieme Verlag: Stuttgart, 1996.
- (3) *Ullmanns Enzyklopädie der Technischen Chemie*, 4th ed.; Verlag Chemie: Weinheim, 1983.
- (4) Kaiya, A. The Use of Natural Squalene and Squalane, and the Latest Situation of the Raw Materials. *J. Jpn. Oil Chem. Soc.* **1990**, *39*, 8.
- (5) Bondioli, P.; Mariani, C.; Lanzani, A.; Fedeli, E.; Muller, A. Squalene Recovery from Olive Oil Deodorizer Distillates. *JAOC* **1993**, *70* (No. 8), 763.
- (6) Catchpole, O. J.; von Kamp, J. C.; Grey, J. B. Extraction of Squalene from Shark Liver Oil in a Packed Column Using Supercritical Carbon Dioxide, *Proc. The 4th International Symposium on Supercritical Fluids, Japan*, 1997; p 175.
- (7) Ruivo, R.; Paiva, A.; Simões, P. Phase equilibria of the ternary system methyl oleate/squalene/carbon dioxide at high pressure conditions. *J. Supercrit. Fluids* **2004**, *29*, 77–85.
- (8) Vázquez, L.; Torres, C. F.; Fornari, T.; Señoráns, F. J.; Reglero, G. Recovery of squalene from vegetable oil sources using countercurrent supercritical carbon dioxide extraction. *J. Supercrit. Fluids* **2007**, *40*, 59–66.
- (9) Buss, D. Gewinnung von Squalen und Squalan aus Olivenöl mittels überkritischer Fluide (H₂ und CO₂) Phasengleichgewichte und Gegenstromextraktion, Dissertation, Technische Universität Hamburg-Harburg: Hamburg, 2000.
- (10) Saure, C. Untersuchungen zur Anreicherung von Squalen und Tocopherolen mittels Gegenstromextraktion mit überkritischem Kohlendioxid, Dissertation, Technische Universität Hamburg-Harburg: Hamburg, 1996.
- (11) Tsang, C. Y.; Streett, W. B. *Phase Equilibria in the H₂/CO₂ System at Temperatures from 220 to 290 K and Pressures to 172 MPa*; Cornell University: New York, 1980.
- (12) Liphard, K. G.; Schneider, G. M. Phase equilibria and critical phenomena in fluid mixtures of carbon dioxide + 2,6,10,15,19,23-hexamethyltetracosane up to 423 K and 100 MPa. *J. Chem. Thermodyn.* **1975**, *7*, 805–814.
- (13) Brunner, G. *Phasengleichgewichte in Anwesenheit komprimierter Gase und ihre Bedeutung bei der Trennung schwerflüchtiger Stoffe*; Habilitationsschrift, Universität Erlangen-Nürnberg: Erlangen, 1978.
- (14) Löhrli-Thiel, H. Die Diffusion von Wasserstoff in Squalan in Abhängigkeit von Druck und Temperatur und die Beeinflussung der Diffusion des Wasserstoffs durch gelöstes Kohlendioxid, Dissertation, Universität Erlangen-Nürnberg: Erlangen, 1978.
- (15) Kim, K. J.; Way, T. R.; Feldmann, K. Th., Jr.; Razani, A. Solubility of Hydrogen in Octane, 1-Octanol, and Squalane. *J. Chem. Eng. Data* **1997**, *42*, 214–215.
- (16) Catchpole, O. J.; von Kamp, J.-Ch. Phase equilibrium for the extraction of squalene from shark liver oil using supercritical carbon dioxide. *Ind. Eng. Chem. Res.* **1997**, *36*, 3762–3768.
- (17) Catchpole, O. J.; Grey, J. B.; Noermark, K. A. Solubility of Fish Oil Components in Supercritical CO₂ and CO₂ + Ethanol Mixtures. *J. Chem. Eng. Data* **1998**, *43*, 1091–1095.
- (18) Sovova, H.; Jez, J.; Khachatryan, M. Solubility of squalane, dinonyl phthalate and glycerol in supercritical CO₂. *Fluid Phase Equilib.* **1997**, *137*, 3762–3768.
- (19) Stoldt, J.; Brunner, G. Phase equilibrium measurements in complex systems of fats, fat compounds and supercritical carbon dioxide. *Fluid Phase Equilib.* **1998**, *146*, 269–295.
- (20) Pfohl, O. Messungen und Berechnungen von Phasengleichgewichten mit nahe- und überkritischem Kohlendioxid sowie assoziierenden Komponenten im Hochdruckbereich, Dissertation, Technische Universität Hamburg-Harburg: Hamburg, 1998.
- (21) Pfohl, O.; Petkov, S.; Brunner, G. *Usage of PE. A Program to Calculate Phase Equilibria*; Herbert Utz Verlag: München, 1998.
- (22) Mathias, P. M.; Klotz, H. C.; Prausnitz, J. M. Equation-of-State mixing rules for multicomponent mixtures: the problem of invariance. *Fluid Phase Equilib.* **1991**, *67*, 31.
- (23) Reid, R. C.; Prausnitz, J. M.; Poling, B. E. *The Properties of Gases and Liquids*; McGraw Hill: New York, 1987.
- (24) Sievers, U. Die thermodynamischen Eigenschaften von Kohlendioxid, Dissertation, Universität Dortmund: Dortmund, 1984.
- (25) Mokbel, I.; Blondel-Telouk, A.; Vellut, D.; Jose, J. Vapor-Liquid Equilibria of two Binary Mixtures: Benzene + n-Tetradecane and Benzene + Squalane. *Fluid Phase Equilib.* **1998**, *149*, 287–308.
- (26) Neubauer, B.; Delhommelle, J.; Boutin, A.; Tavitiyan, B.; Fuchs, A. H. Monte Carlo Simulations of Squalane in the Gibbs Ensemble. *Fluid Phase Equilib.* **1999**, *155*, 167–176.
- (27) Huang, S. H.; Radosz, M. Equation of State for Small, Large, Polydisperse, and Associating Molecules. *Ind. Eng. Chem. Res.* **1990**, *29*, 2284.
- (28) Spano, J. O.; Heck, C. K.; Barrick, P. L. Liquid-vapor equilibria of hydrogen-carbon dioxide system. *J. Chem. Eng. Data* **1968**, *13*, 166–168.
- (29) Bezanahtak, K.; Combes, G. B.; Dehghani, F.; Foster, N. R.; Tomasko, D. L. Vapor-Liquid Equilibrium for Binary Systems of Carbon Dioxide + Methanol, Hydrogen + Methanol, and Hydrogen + Carbon Dioxide at High Pressures. *J. Chem. Eng. Data* **2002**, *47*, 161–168.

Received for review November 30, 2008. Accepted February 14, 2009. The support of DSM Vitamins Ltd. (former F. Hoffmann-La Roche AG) and of the European Union under project NO. EC-Project PL-1075 is greatly acknowledged.

JE800926Z